DOE/MC/29061-96/C0692

CONF-960815--5

MEASUREMENTS OF MEAN FLOW AND EDDY TRANSPORT OVER A FILM COOLING SURFACE

Author:

Ling Wang
Henry Tsang
Terrence Simon
Ernst Eckert

Contractor:

University of Minnesota
125 Mechanical Engineering
111 Church Street, SE.
Minneapolis, Minnesota 55455-0111

Contract Number:

DE-FC21-92MC29061

Conference Title:

National Heat Transfer Conference

Conference Location:

Houston, Texas

Conference Dates:

August 3-6, 1996

Conference Sponsor:

American Society of Mechanical Engineers

Contracting Officer Representative (COR):

Norm Holcombe, C05

DISCLAIMER

To be presented at the
1996 National Heat Transfer Conference
August 3-6, 1996
Houston, TX

MEASUREMENTS OF MEAN FLOW AND EDDY TRANSPORT OVER A FILM COOLING SURFACE

Ling Wang

Henry Tsang

Terrence W. Simon

Ernst R. G. Eckert

Heat Transfer Laboratory

University of Minnesota

Minneapolis, MN 55455, U.S.A.

612-625-5831, Fax: 612-624-5230, e-mail: tsimon@me.umn.edu

ABSTRACT

Results of an experimental study of the effects of blowing Velocity Ratio (VR = 0.5 and 1.0) and Free-Stream Turbulence Intensity (FSTI = 0.5% and 12%) on turbulent transport over a film-cooling test surface are presented. The surface has a single lateral row of streamwise-oriented holes angled 35° from the surface and separated from one another by three hole diameters. The film cooling flow and mainstream flow are at the same temperature and the film cooling is supplied through long delivery tubes. Velocity, turbulence intensity and eddy transport profiles are presented. The ratios of lateral eddy diffusivity to wall-normal eddy diffusivity values measured in this program (4-15) provide documentation of strong anisotropy of eddy transport in the flow.

Nomenclature:

D	diameter of the film cooling holes
FSTI	freestream turbulence intensity ($\sqrt{\overline{u'^2}}/U_o$)
L	length of the film cooling delivery tube
TI%	local turbulence intensity normalized with local mean streamwise velocity ($\sqrt{\overline{u'^2}}/U$)
U	time average streamwise velocity
U_o	time average freestream velocity
$\overline{u'w'}$, $\overline{u'v'}$ and $\overline{v'w'}$	Reynolds shear stresses
V	time average velocity normal to the wall
VR	ratio of film cooling mean velocity to approach velocity at nozzle exit or external to the boundary layer
W	time average lateral velocity
x	streamwise distance from center of the hole
y	distance normal to the test wall
z	lateral distance from center of the middle hole

Greek:

θ	momentum thickness
δ	boundary layer thickness
ε	eddy diffusivity (i.e. $\varepsilon_{Mz} = \overline{u'w'}/(dU/dz)$)

Subscripts:

o	reference location at the centerline of the middle hole
M	momentum

Superscripts:

u', v', w'	instantaneous values of streamwise, wall-normal and lateral velocity fluctuations
$\bar{}$	time-averaged

INTRODUCTION

Film cooling is used to protect a solid wall which is exposed to a high-temperature fluid flow. The technique involves injecting a coolant flow through arrays of holes or slits in the wall into the boundary layer of the high-temperature fluid flowing over the surface. The coolant forms a film along the surface which isolates it from the hot fluid flow. Film cooling is most efficient if the coolant is ejected as a wall jet through a continuous slot (Goldstein, 1971). For practical reasons, a more common geometry is a series of discrete holes. Efficiency of

film cooling depends on the way in which the secondary coolant distributes itself over the surface. The situation is complex due to the interaction between the coolant flow and the mainstream. The major factors that govern this interaction are hole and supply plenum geometry, spacing, injection angle, blowing velocity ratio, pressure ratio, free-stream turbulence intensity and coolant-to-free-stream density ratio. Such a technique is frequently used to cool gas turbine blades. In the present study, measurements within the film cooling flow (as opposed to surface measurements) for cases with in-line injection are presented. In the following, papers from the literature which present results of similar measurements are reviewed.

Cho and Goldstein(1995a,b) present several representative experiments on film cooling related to geometry and spacing of the holes. Kohli and Bogard (1995) investigated the effects of a large angle of injection on the surface effectiveness and measured thermal and velocity fields over the surface. They used a 55° injection angle and compared the results with the traditional 35° case. They found that with the large angle of injection, there was little change in the effectiveness for a low velocity ratio case but a significant decrease in effectiveness with large angle of injection was observed for high velocity ratio cases. Schmidt and Bogard (1995) studied the effect of streamwise pressure gradient on film cooling. They concluded that favorable pressure gradient improved lateral spreading of the jets immediately downstream of the film cooling holes and increased the decay rate of the laterally-averaged effectiveness values when the cooling jets did not completely detach.

Schmidt et al. (1994) evaluated the effect of compound angle injection. At high momentum flux ratios, compound angle injection gave higher effectiveness values than did cooling with streamwise-directed holes. However, the overall performance of the film cooling became poor further downstream. The effect of high freestream turbulence on film cooling effectiveness was documented by Bons et al. (1994). The high freestream turbulence and resultant enhanced mixing reduced film cooling effectiveness by up to 70% in the region directly downstream of the injection hole. At the same time, high free-stream turbulence also produced a 50-100% increase in film cooling effectiveness in the near-hole regions between injection holes.

Since film cooling is strongly dependent upon the free-stream turbulence level, it is desirable to reproduce in the experiment the highly-turbulent free-stream conditions found at the exit of a combustor. Documentation of combustor exit flows is sparce. However, the measurements of Goebel et al. (1993) indicate that FSTI levels of 8-12% are reasonable for combustor exit flow. The choice taken herein is to match the high end of this FSTI range in a facility that is geometrically similar to a combustor/blade combination with the hope that length scales in the facility will be representative of engine conditions.

Most of the existing computational work on heat and mass transfer in the turbulent mixing zone of a film cooling situation is formulated using isotropic diffusion of turbulence. Here, turbulence closure models developed from 2-D boundary layer flows are used to compute the wall-normal eddy diffusivity of momentum, $\varepsilon_{M,y}$ (Patankar et al. 1973). Emerging evidence is showing that the isotropic assumption is not accurate when the flows are three-dimensional. Thus, solution of discrete-hole film cooling flows requires knowledge of the eddy diffusivity in the wall-normal direction as well as in the lateral direction (Sathyamurthy and Patankar, 1990). Some documentation of the magnitude of the lateral diffusivity can be found in the literature. Quarmby and Quirk (1972) measured both circumferential eddy diffusivity and radial diffusivity for flow in a circular tube. They expressed their results as the ratio of circumferential eddy diffusivity to radial eddy diffusivity, finding the ratio to be a single function of non-dimensional radius which rises to values of several hundred as the wall is approached.

Computation plays an important role in modeling film cooling. Leylek and Zerkle (1994) made a comparison between the experimental results and their computational analyses for crossflow of discrete-jet film cooling. Another paper, by Demuren et al. (1986), described their 3-D calculation of film cooling. Three-dimensional computations by Patankar and Spalding (1972) were used by Patankar et al. (1973) to predict slot film cooling effectiveness values. Bergeles et al. (1976 and 1978) used the partially-parabolic, three-dimensional procedure of Pratap and Spalding (1976) to predict discrete hole cooling performance. Demuren and Rodi (1983) applied the locally-elliptic procedure of Rodi and Srivatsa (1980) to alleviate the blowing rate restriction. Demuren et al. (1986) extended the study, using the same procedure, to a variety of cases and obtained reasonable agreement with experimental data. All the above computational efforts were performed using the k-ε, two-equation turbulence model to estimate the Reynolds stress terms in the time-averaged momentum equations. As noted above, film cooling performance computation has been with a finite volume technique and with k-ε turbulence closure. A k-ε formulation with isotropic turbulent eddy viscosity was found to be unsatisfactory for the prediction of the discrete hole film cooling performance, however, as discussed by Sathyamurthy and Patankar (1990). They adopted a modification to this formulation which was proposed by Bergeles et al. (1978) to show an improvement of the accuracy of computation of the spreading of the film cooling jets and the distribution of effectiveness in the lateral direction just downstream of the holes. This anisotropic model gave a distribution of eddy diffusivity ratio as $\varepsilon_{M,z} / \varepsilon_{M,y} = 1 + (3.5(1 - y/\delta))$ where δ is the boundary layer thickness. The anisotropic model was developed from data taken in a fully-developed, turbulent tube flow. This relationship was applied to the entire flow field and to all cases. The present study verifies the anisotropy of the film cooling flow by direct measurement and offers an opportunity to modify this model for more direct application to film cooling calculations.

In this paper, the results of an experimental study of the effect of the film cooling flow on the fluid mixing zone downstream of film cooling injection are presented. This mixing zone is where the film cooling flow and the external flow interact and exchange momentum. Along with mean velocity and turbulence intensity profiles are profiles of eddy diffusivity ratio. The focus of the current experimental research is to provide support for computational development and to document the mixing region flow.

EXPERIMENTAL TEST FACILITY

High-turbulence facility

The high turbulence test facility is a small, open-loop wind tunnel (Fig. 1) which consists of four fans, a jet-interaction zone, a nozzle, and a film cooling test section. The main air flow, supplied by two fans through a settling chamber, is separated into two nearly equal parts (Fig. 2). One part is distributed across the back panel and the other is conducted into the first row of jets in the side panels. These two flows combine to create a recirculation zone inside the turbulence generator. This flow interacts with flow through downstream air jets in the side panels. A contraction with 2.67:1 area ratio (dimensions of the exit area are 68.6 cm x 12.7 cm) is then used to improve the uniformity of the flow to the film cooling test section. A comparison of the measured power spectra of the three components of the velocity (u', v', w'), shows that the flow approaching the film cooling test section is isotropic. The integral length scale calculated from the u' power spectrum is approximately 3.3 cm. The turbulence intensity generated from this wind tunnel for the flow approaching the film cooling test section was measured to be approximately 12%. The essential features of this facility were taken from the works of Ames (1994).

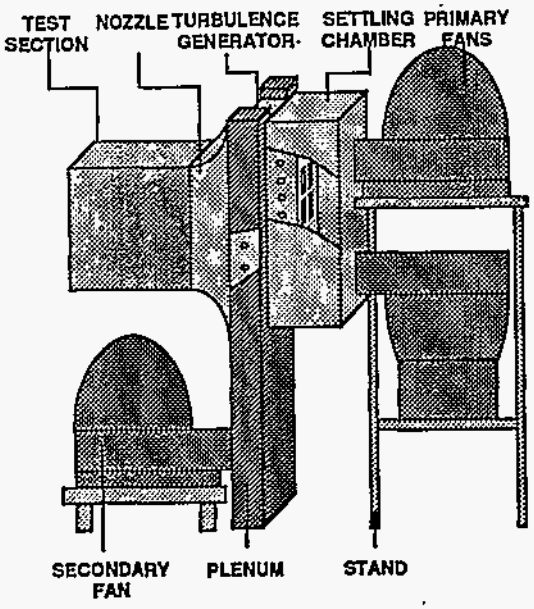

Figure 1 High turbulence facility

Low-turbulence facility

The low turbulence facility is also a open-loop wind tunnel. This is a standard configuration with a fan, screens, a setting chamber, a 6.4:1 area reduction nozzle of exit area 68.6 cm x 12.7 cm, and the film cooling test section. The film cooling test section is the same one used in the high turbulence facility. Turbulence intensity generated from this wind tunnel for the flow approaching the film cooling test section was measured to be approximately 0.5%.

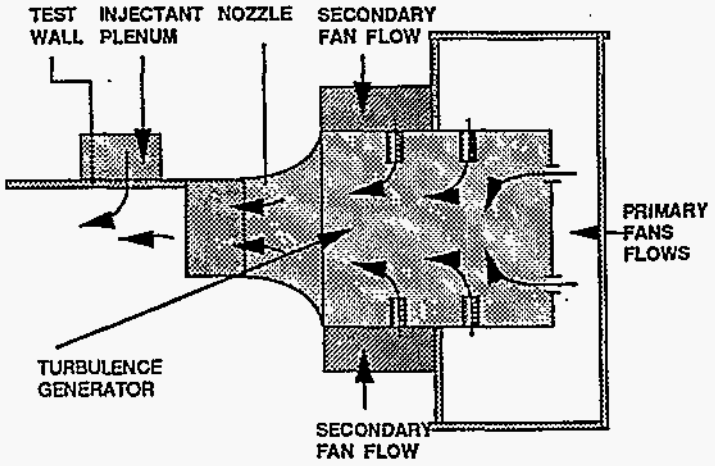

Figure 2 Flow interaction in the high-turbulence facility

Test section

The test section (Fig 3) consists of an upstream plate (25.4 cm x 68.58 cm), the test plate (15.24 cm x 68.58 cm), a downstream plate (91 cm x 68.58 cm), and the film cooling supply system. There is a single column of eleven film cooling holes distributed uniformly on the test plate. The film cooling flow is injected at an angle of 35 degrees in the streamwise direction and 0 degrees in the lateral direction with the film cooling holes machined to a diameter of 1.9 cm (0.75 inch) and positioned three diameters apart, center to center. The film cooling delivery tubes have a length to diameter ratio of 7. This is a sufficient length to establish fully-developed flow within the delivery tube and matches the length to diameter ratio used by Goldstein, Eckert, and Burggarf (1974). Film cooling flow is supplied by a fan through a metering section and a supply plenum which was designed for uniform distribution of flow to the holes.

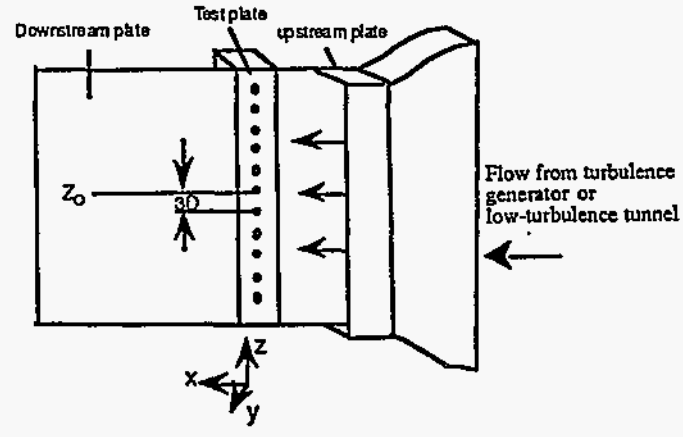

Figure 3 The test section (D is the hole diameter; the reference location, Zo, is the lateral center of the plate)

Instrumentation

Both triple-sensor (TSI model 1294-20) and single-sensor (TSI model 1218-T1.5) hot-wire probes are used to obtain the velocity and turbulence data. They are driven by a TSI-100 bridge unit. The single-sensor probe was used to measure the mean and local turbulence intensity profiles as well as the gradients, dU/dy and dU/dz, whereas the triple-sensor probe was used to measure the Reynolds shear stress data, $\overline{u'w'}$, $\overline{u'v'}$ and $\overline{v'w'}$.

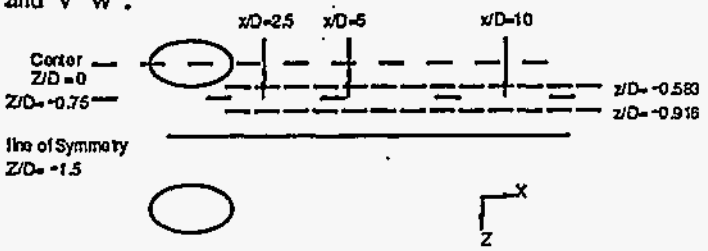

Figure 4. Configuration of the test section showing measurement planes (x-dimension not to scale)

Figure 4 shows the different positions where data are taken. The triple-sensor probe is positioned at z/D = -0.75 and profile data are taken along the y direction (normal to the wall). For gradient evaluation, the single-sensor probe is positioned at z/D = 0.167 above and below the z/D = - 0.75 plane. Differences are used to evaluate dU/dz and mean values are used to find dU/dy. Eddy diffusivity in the z direction is computed as

$\varepsilon_{M_z} = -\overline{u'w'} / (dU/dz)$ and eddy diffusivity in the y direction is computed as $\varepsilon_{M_y} = -\overline{u'v'} / (dU/dy)$. Mean velocity and single-component turbulence intensity profile data are taken also at z/D = 0 and - 1.5.

Experimental uncertainties for measurements of multiple hot-wire probes are difficult to assess. In preparation for the present study, measurements were taken in a fully-developed turbulent pipe flow and were compared against the data of Laufer (1953). As a second comparison, the probe was put in two positions within this flow, one a 90° rotation of the other, and values such as shear stress, $\overline{u'v'}$, from both positions were compared. Based on these comparisons, we can say that Reynolds shear stresses can be measured to within a 5% uncertainty except near the wall ($y/\theta<4$). This is in line with our previous experience with such measurements, with the scatter in the present shear stress data, and with the results of a careful assessment of hot-wire measurement uncertainties by Yavuzkurt (1984). Mean velocities measured with a single wire are with 5 % uncertainty, except very near the wall ($y/\theta < 0.02$). Gradients computed from these single-wire measurements are assigned an uncertainty level of 15 % except where the gradients become excessively shallow (y/θ >11-12). This is consistent with the scatter of the gradient data. These uncertainty values are propagated with the technique of Kline and McClintock (1953) to give an uncertainty for eddy diffusivity of 16 %. Assuming that all entries to the computation are independent, a single-sample uncertainty for the eddy diffusivity ratio of 20 % is computed. If a representative mean value of the ratio is computed for a short range of y/θ from a pool of four values, for instance, the uncertainty of that mean value is the reciprocal of the root of four, or one-half of the single-sample uncertainty (10 %).

EXPERIMENTAL RESULTS

The operating conditions for the various cases examined in this study are given in Tables 1 and 2. All cases were run with a free-stream velocity of 10.8 m/s. The results of these cases are discussed in the following section. The mean velocity and turbulence intensity distributions taken directly in-line with the reference hole (z=zo) at different streamwise locations (upstream and downstream) are shown in Figs. 5 and 6. These two figures show first of all that though the external flow to the film cooled plate is a wall jet shearing on the external flow ($y/\theta > 30$), a uniform velocity and turbulence intensity core flow (which displays a very slow turbulence decay rate in the streamwise direction) can be obtained between the boundary layer and the shear layer, even at x/D=10.0. The boundary layer momentum thickness used for scaling the abscissa increases as x increases (see Table 2). Figures 5 and 6 show strongly disturbed profiles at x/D = 2.5 compared to the upstream profiles at x/D = - 4.0 but a rapid recovery thereafter. These figures are for a low blowing ratio where the streamwise velocity of the injection flow is 40% of the freestream velocity and about 50-60% of the boundary layer flow velocity for the region it most influences. The film cooling flow for this case therefore represents a blockage (compare the upstream profile, x/D = - 4.0, with the first downstream profile, x/D = 2.5). Recovery of the mean profile to standard-shaped profiles requires about 10 diameters of streamwise distance (compare the far downstream profile, x/D = 10 to the upstream profile, x/D = - 4.0).

Figures 7 and 8 show mean velocity and turbulence profiles for x/D = 5.0 but for different lateral positions. They show that at this streamwise position the flow midway between holes is not greatly influenced by the film cooling flow, the flow directly behind the hole is strongly influenced, and the flow between these two, the lateral position near the steepest lateral gradients, is influenced in its unsteadiness but not so much in its mean velocity. The uninfluenced mean velocity profile coincident with the changed turbulence intensity (unsteadiness) profile may be an indication that at this point the film cooling jets are waving from side to side, thus influencing the rms fluctuation of velocity, with little effect on mean velocity. A comparison case for a higher blowing ratio (VR=1.0) is shown in Figs. 9 and 10. Film cooling flow shoots into the boundary layer first, then spreads to cover the test section surface. Contrary to Fig. 7,

Table 1 Flow parameters for upstream position and comparison cases (U_o = 10.8 m/s)

VR	T.L.	z/D	x/D	Cf ($\times 10^3$)	x/θ	Reθ
0	12%	0	- 4.0	5.7	- 143	495
0.5	12%	0	5	3.6	43	2035
0.5	12%	1.5D	5	5.1	101	878

Table 2 Profile data (U_o = 10.8 m/s)

VR	T.I.	x/D	C_f (x10^3)	y/θ	$\varepsilon_{M,x}/\nu$	$\varepsilon_{M,y}/\nu$	$\varepsilon_{M,z}/\varepsilon_{M,x}$	x/θ	Reθ
0.5	12%	2.5	6.5	5	365	1.67	218	100	885
				6	387	26.2	14.8		
				7	432	35.3	12.3		
				8	690	67	10.3		
				9	1058	71	15		
				10	3850	128	30		
				11	1026	154	6.7		
				12	916i	145	63		
0.5	12%	5	4.8	1.5	140	14	6.8	73	1212
				2.2	253	27	11		
				3	342	21	9.		
				3.6	461	32	14.5		
				4.4	602	51	6		
				5.1	610	105	5.8		
				5.8	603	116	7.7		
				6.6	756	116	7.4		
				7.3	667	118	4.7		
				8	1003	146	10		
				8.7	926	119	6.		
				9.5	858	112	9.6		
				10	1531	250	9		
0.5	12%	10	4.7	1.2	2534	22	117	60	1478
				1.8	896	36	25		
				2.4	1102	63	17.6		
				3	1184	85	14		
				3.6	1515	106	14.3		
				4.2	983	146	6.7		
				4.8	1008	127	7.9		
				5.4	1720	174	10		
				6	878	216	4		
				6.6	785	237	3.3		
				7.2	2115	192	11		
1	12%	5	5.8	5	325	33	10	249	354
				7.5	345	50	6.8		
				10	406	59	6.9		
				12.5	647	93	6.9		
				15	1218	64	19		
				17	1058	120	8.8		
				20	-2612	-122	21		
0.5	2%	5	4.4	2.3	1066	16.7	64	78	1136
				3.1	114	14.2	8		
				3.9	71	15.5	4.6		
				4.7	74	21	3.5		
				5.4	78	20	3.8		
				6.2	68	15.5	4.4		
				7	75	13	5.7		
				7.8	66	15.7	4.2		
				8.5	66	11.3	5.8		
				9.3	93	12	7.8		
				10	107	11.6	9.2		
				10.9	88.8	8.2	10.8		

which shows a blockage due to the film cooling flow, Fig. 9 shows an acceleration of the near-wall flow. For this case with a velocity ratio of 1.0, the streamwise component of the film cooling flow is about 80% of the freestream velocity and 100-120% of the boundary layer velocity in the region which it influences most. Thus, in this case, the film coolant tends to

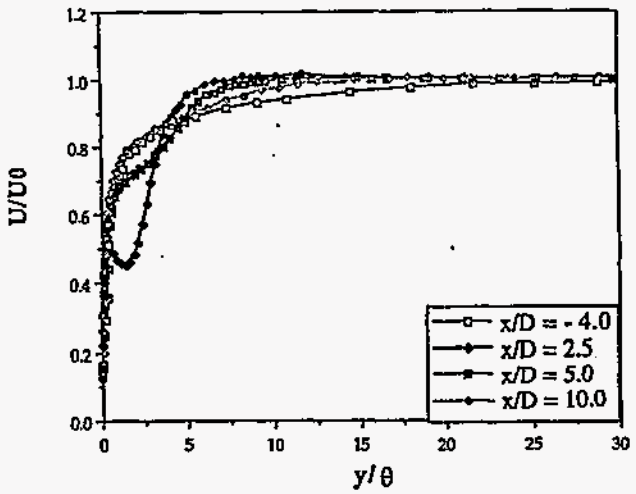

Figure 5 Velocity distribution at VR=0.5, z=z_o, FSTI=12%

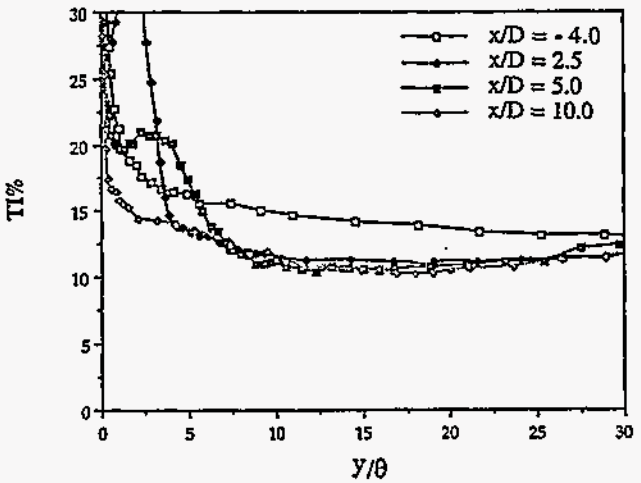

Figure 6 Turbulence distribution at VR=0.5, z=z_o, FSTI=12%

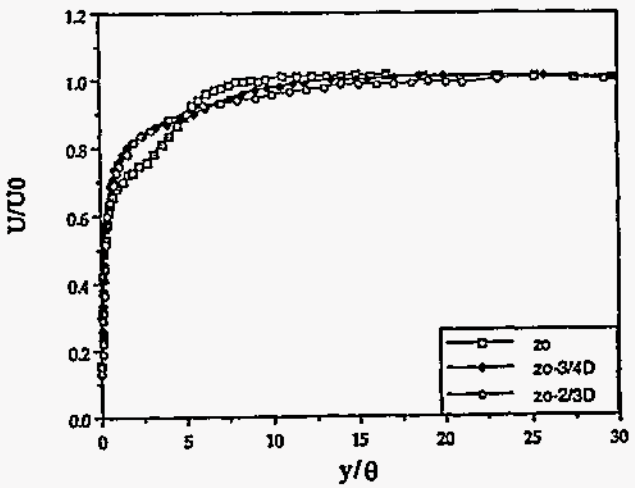

Figure 7 Velocity distribution at VR=0.5, x/D=5, FSTI=12% for three z-planes (locations are in Figure 4)

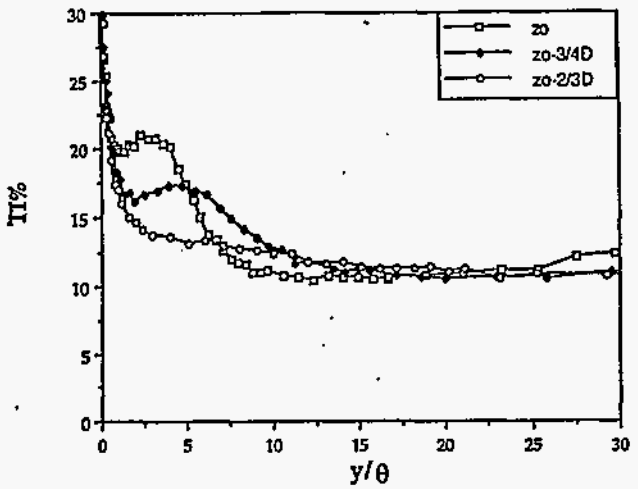

Figure 8 Turbulence distribution at VR=0.5, x/D=5, FSTI=12% for three z-planes (locations are in Figure 4)

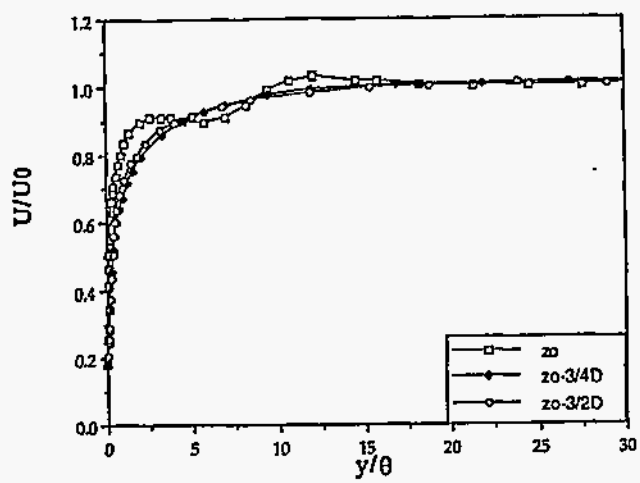

Figure 9 Velocity distribution at VR=1, x/D=5, FSTI=12% for three z-planes (locations are in Figure 4)

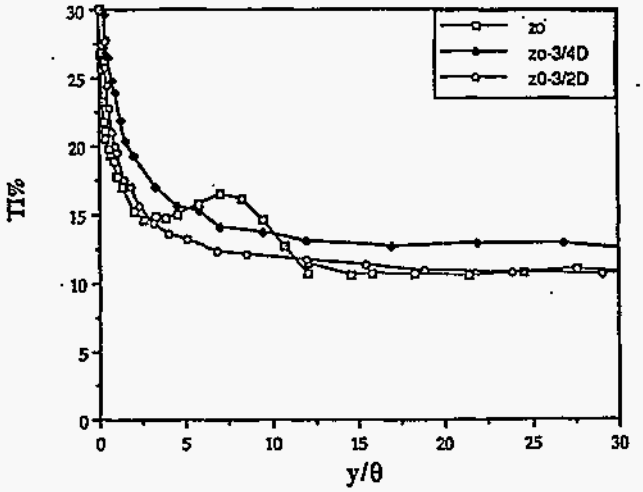

Figure 10 Turbulence distribution at VR=1, x/D=5, FSTI=12% for three z-planes (locations are in Figure 4)

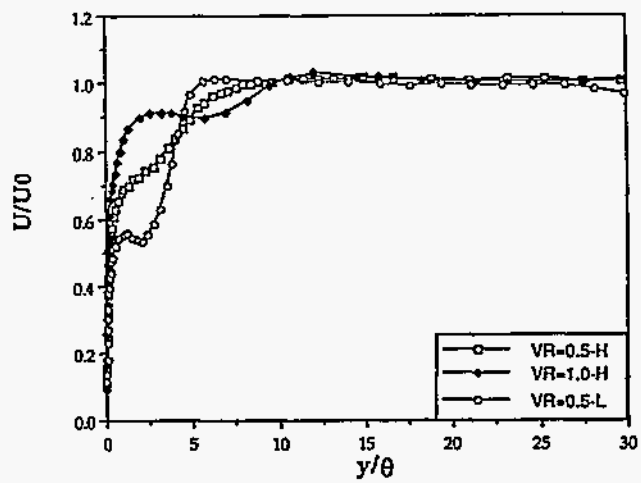

Figure 11 Velocity distribution at x/D=5, z= z_o (H=12% FSTI, L=0.5% FSTI)

accelerate the boundary layer flow. A comparison of Figs. 7 and 9 for mean velocity and Figs. 8 and 10 for turbulence intensity shows that the VR=1.0 coolant jet influences the turbulence level only directly behind the hole and not significantly at other lateral planes. A direct comparison of the VR=0.5 and VR=1.0 flows under high turbulence intensity conditions can also be seen in Figs. 11 and 12. Here, only the flows directly behind the holes are compared. The acceleration of boundary layer flow by film cooling flow and the deeper penetration of the VR=1.0 flow are visible in Fig. 11 and lesser near-wall shear and deeper penetration of the VR=1.0 flow are visible in Fig. 12.

Figures 11 and 12 also show the effect of free-stream turbulence intensity on the flow which is five diameters downstream of the film cooling holes. Because lateral spreading of the jet in the low-turbulence intensity flow is reduced, its effect as a near-wall flow blockage is increased. Perhaps this blockage is the source of the far-field (5< y/θ <7) flow acceleration relative to that of the High-FSTI flow. Figure 12 would indicate that the near-wall flow (y/θ ~ 2, Fig. 12) is rather quiet but the turbulence in the region of steeper shear (y/θ ~ 3-4) is more active. Overall, it is clear that elevated free-stream turbulence intensity has a marked effect on the film cooling mixing zone. Figures 11 and 12 also show the effect of velocity ratio when the FSTI is high. Again, a core flow region (12 < y/θ < 20) which is uninfluenced by the film cooling flow, the boundary layer, or the external free shear layer is visible for each case.

Figures 13 and 14 show the velocity gradients and $\varepsilon_{M_z} / \varepsilon_{M_y}$ ratio profiles for VR=0.5 and FSTI = 12% at different x/D positions. The eddy diffusivity values are computed as

$\varepsilon_{M_z} = -\overline{u'w'} / (dU/dz)$, $\varepsilon_{M_y} = -\overline{u'v'} / (dU/dy)$, thus large variations exist whenever the gradients become weak (see Fig. 13). Values of ε_{M_z}, ε_{M_y}, and their ratio are given only where the gradients are sufficiently steep for accurate evaluation. The eddy diffusivity ratio data (Fig. 14) show a mild drop from 12-

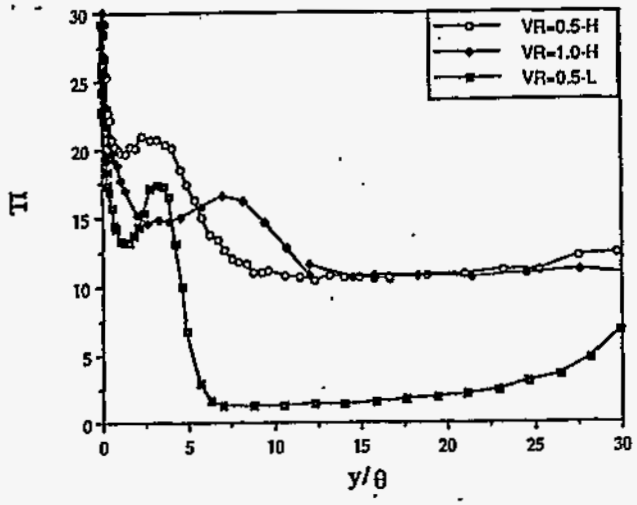

Figure 12 Turbulence distribution at x/D=0.5, z=z_o for two velocity ratios and two FSTI (H=12% FSTI, L=0.5% FSTI)

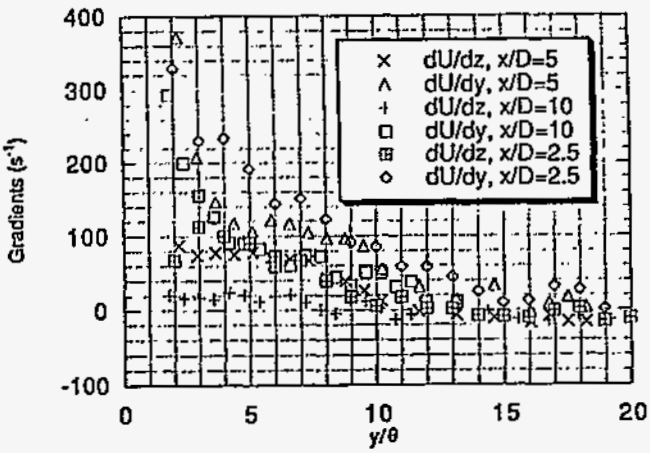

Figure 13 Velocity gradients at different x/D ratio (VR=0.5, FSTI=12%)

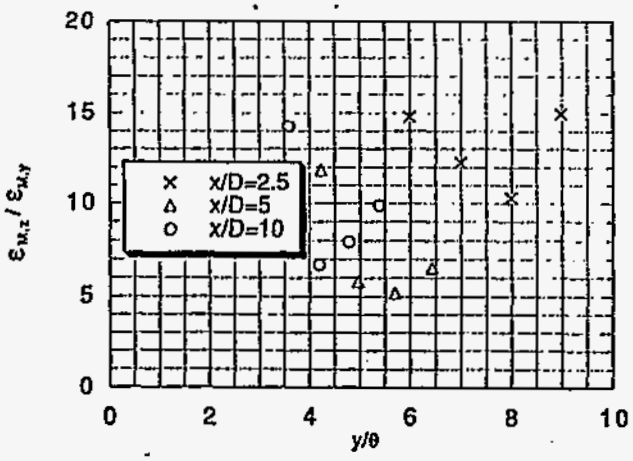

Figure 14 Eddy diffusivity ratio at different x/D ratio (VR=0.5, FSTI=12%)

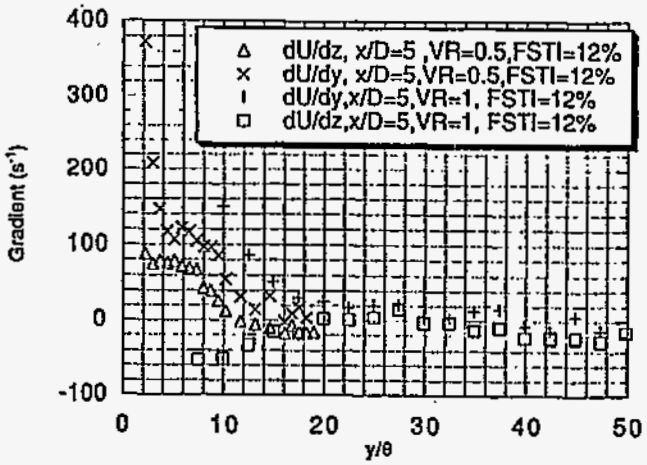

Figure 15 Velocity gradients at different VR (z/D=3/4)

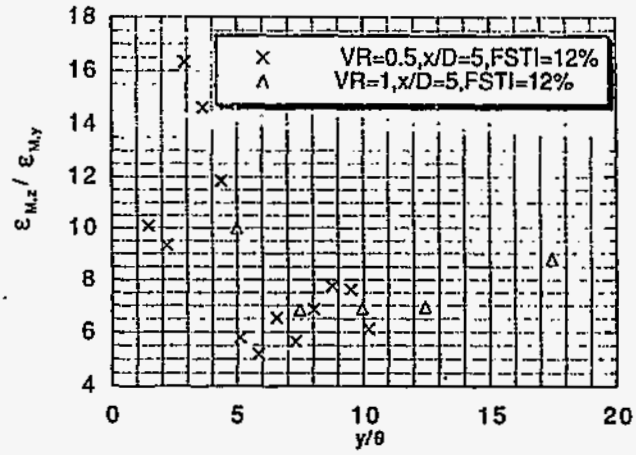

Figure 16 Eddy diffusivity ratio at different VR (z/D=3/4)

13 at x/D = 2.5 to 6.0 at x/D = 5 and then a rise to 8-9 at x/D = 10. Considering the single-sample uncertainty for these values of 20%, the slight rise between x/D = 5.0 and x/D = 10.0 may not be significant. The data do show that, generally, eddy transport in the lateral direction is approximately 5-15 times as effective as eddy transport normal to the wall.

Figures 15 and 16 show the velocity gradients and the $\varepsilon_{M,z}$ / $\varepsilon_{M,y}$ ratio profiles for the two velocity ratios where x/D = 5.0 and FSTI = 12%. Figure 15 shows that values of dU/dy increase from the VR=0.5 case to the VR=1.0 case. This is mainly due to the increase in streamwise momentum of the air flow from the film-cooling holes for the VR=1 case. The near-wall values of dU/dz become negative as a result of the strong blowing in the VR=1 case. Also, the streamwise velocity of the film cooling flow is actually larger than the main flow velocity at this point. For the VR=0.5 case, the air from the film-cooling holes blocks the main air flow and dU/dz is positive. In Fig. 16, one can see that the eddy diffusivity ratios of these two cases are nearly the same. It appears, therefore, that the eddy diffusivity ratio does not depend strongly on velocity ratio.

Figures 17 and 18 show the velocity gradient and $\varepsilon_{M,z}$ / $\varepsilon_{M,y}$

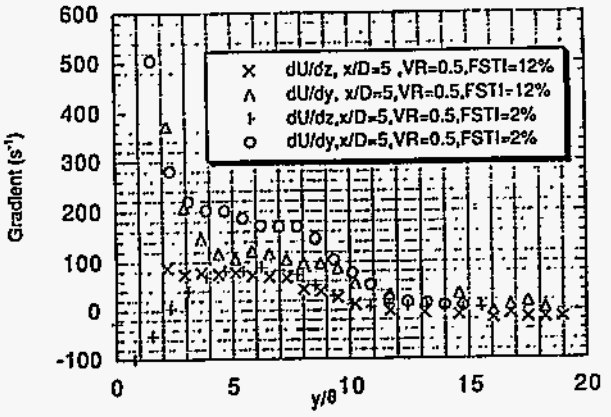

Figure 17 Velocity gradients at different turbulence intensity

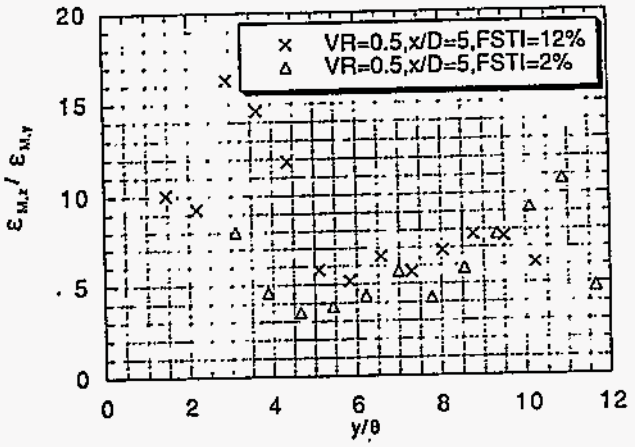

Figure 18 Eddy diffusivity ratio at different turbulence intensity

ratio profiles at different free-stream turbulence intensity values for x/D = 5.0 and VR = 0.5. The velocity gradients, dU/dz, are similar and dU/dy are stronger for the higher FSTI. The effect on eddy diffusivity ratio is shown in Fig. 18. The values appear to be generally larger in the FSTI = 12% case than in the FSTI = 0.5% case. However, the difference is small and of nearly the same size as the magnitude of the data scatter.

CONCLUSIONS

The effects of turbulence intensity and blowing velocity ratio on the turbulence transport over the film-cooled test surface are investigated. The measurements were carried out utilizing two wind tunnels, one with a 12% FSTI and the other with a 0.5% FSTI. Velocity, local turbulence intensity, and eddy diffusivity ratio profiles are presented at different streamwise and lateral positions and with different blowing ratios for comparison. The following conclusions are drawn.

•The film cooling flow with VR=0.5 acts like an obstacle to the main flow. The effect is diminished after 10 diameters of streamwise distance in a high FSTI mainstream flow. Due to the addition of the film cooling flow, the velocity is decreased and the turbulence intensity is increased in the region where the film cooling flow and mainstream flow mix.

•The situation changes considerably with increased VR in that the boundary layer flow is actually accelerated by the film cooling flow when VR=1.0.

•Eddy transport is considerably larger in the lateral direction than in the wall-normal direction for all the locations and conditions investigated. The eddy diffusivity ratio $\varepsilon_{M,z} / \varepsilon_{M,y}$ is in the range 4-15.

•The eddy diffusivity ratio decreases with streamwise distance in the near vicinity of the injection holes and tends to approach an asymptotic value with streamwise distance at x/D=5.0.

•The eddy diffusivity ratio seems to not depend significantly on velocity ratio.

•The eddy diffusivity ratio appears to depend weakly on turbulence intensity of the main flow. It increases slightly with an increase in turbulence intensity from 0.5% to 12%.

ACKNOWLEDGMENTS

This work is a base-case for studies on film cooling with short-hole delivery and on film cooling with lateral injection sponsored by NASA-Lewis Research Center and DOE, respectively. The DOE project is managed by Dr. Danial Fant of the South Carolina Energy R&D Center and the NASA study Project Monitor is Douglas Thurman.

REFERENCES

Ames, F.E., 1994, "Experimental study of vane heat transfer and aerodynamics at elevated level of turbulence", NASA contractor report, CR-4633.

Bergeles, G., Gosman, A.D., and Launder, B.E., 1976, "The prediction of three-dimensional discrete-hole cooling processes, Part 1 - Laminar flow," ASME J. Heat Transfer, Vol.98, No. 3, p.379.

Bergeles, G., Gosman, A.D., and Launder, B.E., 1978, "The turbulent jet in a cross stream at low injection rates: A three dimensional numerical treatment," Num. Heat Transfer, Vol.1, p. 217.

Bons, J.P., MacArthur, C.D., and Rivir, R.B., 1994, "The effect of high freestream turbulence of film cooling effectiveness," ASME paper 94-GT-51.

Cho, H.H. and Goldstein R.J., 1995a, "Heat (mass) transfer and film cooling effectiveness with injection through discrete holes. Part I: with holes and on the back surface," ASME J. of Turbomachinery, vol. 117, pp. 440-450.

Cho, H.H. and Goldstein R.J., 1995b, "Heat (mass) transfer and film cooling effectiveness with injection through discrete holes. Part II: on the exposed surface," ASME J. of Turbomachinery, vol. 117, pp. 451-460.

Demuren, A.O. and Rodi, W., 1983, "Three-dimensional calculation of film cooling by a row of jets," Notes Num. Flu. Mech., Vol.7, p.49.

Demuren, A.O., Rodi, W., and Schonung, B., 1986, "Systematic study of film cooling with a three-dimensional calculation procedure, " ASME J. of Turbomachinery, vol. 108, p. 124

Goldstein, R.J., 1971, "Film cooling," Advances in Heat Transfer, Vol. 7, Academic Press, p.321-379

Goldstein, R. J., and Eckert, E. R. G., Burggarf, F., 1974, "Effects of hole geometry and density on three-dimensional film cooling," Int. J. Heat Mass transfer, vol. 17, p. 595.

Goebel, S. G., Abuaf, N., Lovett, J. A., and Lee, C.-P., 1993, "Measurements of Combustor Velocity and Turbulence Profiles," ASME Paper 93-GT-228.

Jubran, B. and Brown, A., 1985, "Film cooling from two rows of holes inclined in the streamwise and spanwise directions," ASME J. of Engineering for Gas Turbine and Power, Vol. 107, p. 84.

Kline, S. J., and McClintock, S. J., 1953," Describing uncertainties in single-sample experiments,"Mechanical Engineering. Jan.

Kohli, A. and Bogard, D.G., 1995, "Adiabatic effectiveness, thermal fields, and velocity fields for film cooling with large angle injection," ASME paper 95-GT-219.

Laufer, 1953," The structure of turbulence in fully developed pipe flow," NACA report 1174.

Leylek J.H. and Zerkle R.D., 1994, "Discrete-jet film cooling: A comparison of computational results with experiments," ASME J. of Turbomachinery, vol. 116, p. 358.

Patankar, S.V. and Spalding, D.B., 1972, "A calculation procedure for heat, mass and momentum transfer in three-dimensional parabolic flows," Int. J. Heat Mass Transfer, Vol. 15, p. 1787.

Patankar, S.V., Rastogi, A.K. and Whitelaw, J.H., 1973, "The effectiveness of three-dimensional film-cooling slots - II. Predictions," Int. J. Heat Mass Transfer, Vol. 16, p. 1673.

Pratap, V.S., and Spalding, D.B., 1976, "Fluid flow and heat transfer in three-dimensional duct flows," Int. J. Heat Mass Transfer, Vol. 19, p. 1183.

Quarmby A. and Quirk R., 1972, "Measurements of the radial and tangential eddy diffusivities of heat and mass in turbulent flow in a plain tube," Int. J. Heat Mass Transfer, Vol. 15, p. 2309.

Rodi, W. and Srivatsa, S.K., 1980, "A locally elliptic calculation procedure for three-dimensional flows and its application to a jet in cross-flow," Comp. Mech. App. Mech. Eng., Vol. 23, p. 67.

Sathyamurthy, P. and Patankar, S.V., 1990, "Prediction of film-cooling with lateral injection," Heat Transfer in Turbulence Flows, ASME-HTD, Vol. 138, p. 61.

Schmidt, D.L., Sen, B., and Bogard, D.G., 1994, "Film cooling with compound angle holes: Adiabatic effectiveness," ASME paper 94-GT-312.

Schmidt, D.L. and Bogard, D.G., 1995, "Pressure gradient effects on film cooling," ASME paper 95-GT-18

Yavuzkurt, S., 1984, "A guide to uncertainty analysis of hot-wire data," J. Fluids Engineering, June, vol. 106, p. 181.